SMGroup

SM Journal of Biomedical Engineering

Research Article

Assessment of Potential Fracture of the Femur's Nick during Fall for Different Bone Densities

Fadi Alkhatib[1], Adeeb Rahman[2] and Mustafa Mahamid[3]*

[1]*Mechanical Engineering Department, Australian College of Kuwait, Kuwait*
[2]*Department of Civil Engineering & Mechanics, University of Wisconsin Milwaukee, USA*
[3]*Department of Civil & Material Engineering, University of Illinois at Chicago, USA*

Article Information

Received date: Jul 25, 2018
Accepted date: Aug 20, 2018
Published date: Aug 24, 2018

***Corresponding author**

Mustafa Mahamid, Department of Civil & Material Engineering, University of Illinois at Chicago, 842 W. Taylor St., Chicago, IL 60607, USA, Tel: 312-355-0364; Email: mmahamid@uic.edu

Keywords Femur's neck; Bone density; Fall; Bone fracture; Finite element analysis

Abstract

Elder men and women are at high risk of falling due to loss of coordination, poor vision, or weak bone structure. The fall can result in sustaining immobilizing fracture. The hypothesis examined in this paper is that fracture can be directly related to bone density alteration in the elderly. To assess the risk and provide understanding for working towards fracture preventive measures, an understanding of the magnitude of stresses and strains and their distribution in anatomical geometric locations in the femur are critical.

Finite element software, ANSYS, was used to predict the stress, strains, and fracture possibility in the neck of a 445-mm long femur bone, and 14.5-mm canal diameter due to sideward fall.

Different bone densities are studied representing healthy to poor density conditions. This study serves to answer the hypothesis as to whether bone density loss had a direct adverse correlation to fracture during a fall event in the elderly. Such findings provide potential future preventive measures for designing devises that can be worn by elderly at risk of fracture in a fall event due to poor bone density. This study introduces a first step in answering the question addressing the correlation of fracture and bone density.

Introduction

Bone is a structural and a metabolic tissue. Its structural functions include providing support for the body against gravity, and static and dynamic loadings. It also acts as a rigid lever system for the muscular action, and serves as a protective covering for the vital internal organs such as the heart, brain, and blood forming marrow. The primary metabolic function of bone lies in the ability to serve as a repository to calcium, which is necessary for nerve conduction, muscle contraction, clot formation, and cell secretion. Evidence is also accumulating to suggest that bone plays a major role in the induction of hemopoietin marrow [1]. A study done by Milovanovic et al. [2] suggests that bone fragility is highly affected by age which in turns increases the risk of fractures. The study shows that the femoral neck fracture is among the highest rates of fracture and is highly affected by age and gender of the patients. The study used atomic force microscopy (AFM) for imaging and mechanical characteristics of bone material specially the femur neck of women at various ages. The aim of the AFM procedure is to investigate the effect of age on bone elasticity and get a better idea of age related bone fragility. Miriam et al. [3] investigated obesity and osteoporosis on adults in the United States. Osteoporosis is a disease that increases fracture risk due to the reduction of bone quantity and quality. The study suggests that more than 20 million adults over the age of 50 meet the criteria of osteoporosis diagnoses. This phenomenon has a direct impact on the femoral bone fracture due to side fall. In a study presented by Koletsi et al. [4], it showed that the cancellous bone structure with plates oriented directly parallel to the sagittal plane is the optimum configuration for femur's strength. This particular configuration provides the bone with the strength to withstand the compressive and tensile strains developed along the sagittal axis. The study suggests that bone loss and number of structural changes of the cancellous bone have been identified. The trabecular morphology of the cancellous bone is determined by the distribution of the stress and strain which leads to a direct impact on the mechanical properties of the bone tissue.

Background and Literature Review

In a study done by Taylor et al. [5], cadaver bones were CT (contiguous tomography) scanned. The natural frequency of the bone was measured using modal analysis technique. A finite element model of the bone was obtained from the CT scan geometries. The mesh was developed with a density distribution established by comparing the mass of the cadaver bone with the mass generated from the finite element model. The orthotropic elastic constants were established by matching the FE predicted values from the modal analysis with the values that are generated from the experimental natural frequency study. A very high degree of correlation was found for both the dense and the

axial Young's modulus (E_{3max}), both with < 1% error. Other material properties had higher error, with a maximum error of 62% found for the Poisson's ratio ν_{12}. The more significant stiffness constants (E_{1max}, E_{2max}, E_{3max}, G_{12max}, G_{13max}, and G_{23max}) showed a maximum of 25% error.

In the study by Stain et al. [6], the author suggested, as it is widely accepted, that with age there is a significant decrease of bone mass combined with a loss of strength. The decrease in mass was correlated by the change in the cross-sectional area. The cross-sectional geometry measurements included the areas and second moment of area for 107 specimens of human femurs aged 21-92 years. A mathematical model was developed, which considered the variations in the bone geometry in relation to age. Specimens of femur bones were taken for different sexes, weights, and heights. The study found that there was a loss in the cross-sectional area with age, and bone tissue was redistributed to resist the stresses in the coronal plane. Another finding was that the torsional stresses were higher in the older femurs than the younger femurs. Furthermore, it was found that for all ages, women had higher stresses, smaller bones, and less cortical area than men.

In a study done by Keyak et al. [7], the authors presented a finite element analysis. This included four models of the femur to predict the force directions that may cause the lowest possibility of fracture. The force directions were varied in the 3-dimensional space for two loading configurations. One configuration represented normal daily activities (atraumatic loading), and one represented falls (traumatic loading). It was found that the traumatic fall configuration led to the greatest risk of fracture, regardless of the load direction.

A study completed by Keyak et al. [8], the authors examined the performance of nine stress and strain based failure theories, "six of which can account for the differences in tensile and compressive material strengths. The distortion energy, Hoffman and Hoffman strain–based analog, maximum normal stress, maximum normal strain, maximum shear strain, maximum shear stress, Coulomb-Mohr, and modified Coulomb-Mohr theories were examined. It was found that the distortion energy theory and maximum shear stress failure theory were the most robust. However, regardless of the failure theory used, whether it was complicated or simple theory dependent on strain, the results were very close.

In a study by Sabick et al. [9], the researchers measured the impact force on the hip and shoulder as a result of falling on the side from a kneeling position. All the subjects fell onto a force platform covered with foam padding in order to measure the impact force. There were three different fall possibilities that were studied; the first one was attempting to break the fall by using an arm, the second one was falling with the body relaxed, and the third one was falling with the body tensed. It was found that the impact forces on the hip and shoulder joints were reduced in the side fall where there was active response. It was found that the possibilities of hip fractures that occur in elderly people are much higher than the fractures that occur in younger people. This is due to the decrease in the reaction time and strength with age.

In a study by Morgan and Keaveny [10], the research team investigated the assumption that the yield strain of human trabecular bone depends on anatomic site. The uniaxial tensile and compressive yield properties were compared with cylindrical specimens taken from the vertebra, proximal tibia, femoral greater trochanter, and femoral neck. These specimens were taken from 61 donors aged 67±15 years. In the test, it was important to minimize the end artifacts. The specimens were loaded along the main trabecular orientation. It was found that the compressive yield strain was higher in the femoral neck than all other sites. Another finding was that the yield strains of the human cortical bone may change from one site to another. On the other hand, the yield strain may be considered to be uniform within a given site, despite the changes in the elastic modulus and yield strain.

In this research, a 3-D finite element model of the femur bone was constructed and used to predict stresses, strains, bone fracture and its location. The FEA model was used to generate stress and strain fields of the entire femur's head; also, to monitor stress and strain distribution on the anterior, lateral, medial and posterior sides of the femur's neck. The FEA model was utilized to study the effect of side fall on the human femur and the effect of various assumptions on boundary conditions, and bone density incorporating the orthotropic nature of human bone.

Model Development

Usually, experiments are used as a main tool in research to study the behavior of structures. Occasionally, this is not feasible due to the risk associated with the experiments, or time and money consumption. Because experiments are not always possible, computational methods are an important tool in predicting the behavior of structures. The major objective of this project was to construct a 3-dimensional finite element model capable of predicting the behavior of femur bone when it was subjected to sideward fall; bone density was also incorporated as part of the study.

The geometry was imported as an IGES formatted file to ANSYS (finite element software) [11,12]. Various volumes describing the orthopedic nature of the human bone were created. These volumes included the outer cortical bone and the inner spongy bone, and the femur canal, as shown in Figure 1.

In Table 1, the cross-sectional areas of the cortical bone, spongy bone, and the gross area of the specified section are available. Figure 2 represents a schematic diagram of the anterior side of the femur bone. In the figure, all the cross sections are shown, with the data available in Table 1.

Meshing

Meshing is an important and vital tool in ensuring the accuracy of the model, since the quality of the results depends on the quality of the mesh. A fine mesh is desired to model the critical areas. Coarse mesh is adequate for non-critical areas to improve computational efficiency. In this femur model, the area of interest was the femur's head. At this location, the results were most important, and the boundary conditions were applied. Therefore, it has a finer mesh while the rest of the femur has a coarser mesh as shown in Figure 3.

Material Properties

The femur's bone consists of two distinct layers: cortical and spongy bone. In this model, cortical bone was modeled as an orthotropic material. The major axis was the inferior superior axis, which is represented by the z axis in this model.

Since bone density varies with respect to age and sex, and the modulus of elasticity depends on the bone's density, it follows that the modulus of elasticity varies with aging. The relation between the modulus of elasticity and bone density for cortical bone is shown in Figure 1 below.

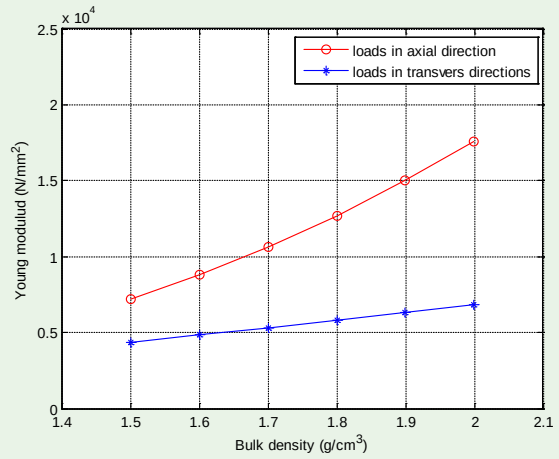

Figure 1: Bone density relationship [13].

The relation between the bone density and modulus of elasticity of the cortical bone is approximated by Equations 1 and 2.

$$E_1 = 2065\rho^{3.09} \quad (1)$$

$$E_2 = 2314\rho^{1.57} \quad (2)$$

Equation 1 approximates the relation of bone density and modulus of elasticity for the cortical bone in the axial load direction. Equation 2 approximates the relation of the bone density and modulus of elasticity for the cortical bone in the transverse load direction. The values of modulus of elasticity and bone density in all cases are shown below in Table 1 below and Table 2 of the supplement to this article:

A sensitivity study was performed, to examine the validity of the assumption that impact loads on the greater trochanter transfer to equivalent loads at the hip joint. Different cases of sideward fall were considered.

The loads on the femur bone shown in Figure 4 were applied as a concentrated load to the femur's head. In this study, there were three loading conditions: A Relaxed condition (falling with the body relaxed, i.e. falling unexpectedly), the Tensed condition (falling with the body tensed i.e. anticipated fall), and the Slap condition; attempting to break the fall by extending an arm. The forces generated in the x, y, and z directions for different fall conditions are shown in Table 2. The values of the impact loads were obtained from a previous study of sideward fall conducted by Sabick et al. [9]. In that study, the ground reactions during fall were measured to determine the impact loads on the hip joint, in terms of body weight, for the above three cases. Data in this study were adopted from Sabick's et al. study.

The loads' angles, which are measured with respect to the longitudinal direction of the shaft (z-axis), and the anterior posterior direction (y-axis) in this FE model, were changed according to the orientation and fall type shown in Figure 2 below [13].

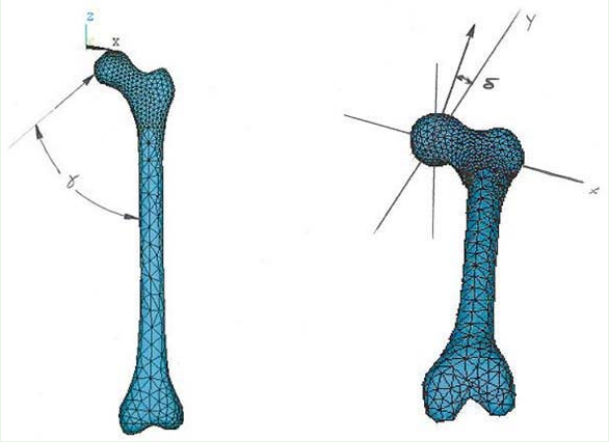

Figure 2: The force angles γ and δ.

Table 1: Material properties and densities for the cortical bone.

Cortical Bone									
r(g/cm³)	Modulus of Elasticity (N/mm²)								
	E_z	E_x	E_y	G_{xy}	G_{xz}	G_{yz}	n_{xy}	n_{xz}	n_{yz}
1.5	7228.4	4373.47	4373.47	2409.47	1669.26	1669.26	0.5	0.31	0.31
1.7	10641.61	5323.14	5323.14	3547.2	2031.73	2031.73	0.5	0.31	0.31
1.8	12697.32	5822.92	5822.92	4232.44	2222.49	2222.49	0.5	0.31	0.31
2	17583.4	6870.38	6870.38	5861.13	2622.28	2622.28	0.5	0.31	0.31

Boundary Conditions

Boundary conditions are an important and critical issue in finite element modeling, since it can affect the output results. In this model, possible sites were chosen as the fixed areas and studied. The effect of changing the boundary conditions was investigated and related to the stress, strain fields, and fracture possibilities.

To investigate the sideward fall, impact loads have been applied to the femur's head and to the greater trochanter. Ideally, dynamic transient analysis would be used to simulate the real fall case as the stresses and strains evolve in time. However, since the wave speed of bone is very great, the required time step in the FEA computation is very small, leading to numerical errors and very long simulation times. Since the rate of load application is slow with respect to the

Table 2: Fall cases, forces generated due to fall [9].

Forces on the Hip Joint (Sideward Fall)					
Condition	Impact Force at Hip Joint	F	F_x	F_y	F_z
	(B.W)	(N)	(N)	(N)	(N)
Relaxed	2.69	2243.06	1669.58	1286.56	767.17
Tensed	2.76	2301.43	1713.03	1320.04	787.13
Slap	2.44	2034.59	1514.42	1167	695.87
γ = 70°		δ = 55°			

wave speed traveling in the bone, Quasi – Static analysis was justified and performed in this study. Load and angle variations for the tensed case are shown in Tables 3 and 4 below:

Table 3: Loading variation due to tensed fall, bone density = 2.0 g/cm³.

Forces on the Hip Joint (Tensed - 2.0)				
Case #	F	F_x	F_y	F_z
	(N)			
1	2301.43	1713.03	1320.04	787.13
2	2301.43	1424.32	1627.35	787.13
3	2301.43	1931.58	972.62	787.13
4	2301.43	1493.29	1320.04	1150.71
5	2301.43	1842.37	1320.04	399.64

Table 4: Angle variation due to tensed fall, bone density = 2.0 g/cm³.

Angle Variation (Tensed-2.0)			
Case #	Angle (deg.)		
	γ	*δ*	θ_x
1	70	55	41.90
2	70	45	51.77
3	70	65	32.93
4	60	55	49.54
5	80	55	36.82

Results

In this study, a femur bone model has been investigated during fall using finite element analysis. Three major fall configurations were studied by simulating these different configurations in an investigation by Sabick et al. [9]. In these cases, the loads were applied at the femur head. Part of the greater trochanter region was modeled as a fixed end. In all the fall configurations, four different bone densities were taken into consideration. For the case of tensed fall, sensitivity analysis study was performed to investigate the effect of varying the load angles on the stress, strain, and fracture as well. One case was studied to examine the effect of swapping the location of the applied load with the location of the applied boundary conditions.

Variation of Density

In the three fall configurations, where the body falls in a different manner, four different densities were investigated (ρ = 1.5, 1.7, 1.8, and 2.0 g/cm³) [14]. Stress and strains were computed from the analysis, the failure prediction scheme was developed using the Maximum Normal Strain theory, Hoffman theory, and Coulomb Mohr theory. Four paths along the femur's neck designating critical neck regions were identified: the anterior side, posterior side, lateral side, and medial side.

In the first failure criteria, failure was projected to occur if the maximum normal strain is equal or exceeds the yielding strain of the bone, per Equation 3:

$$\frac{\varepsilon_1}{\varepsilon_{yielding}} = 1,\ \varepsilon_1 \rangle \varepsilon_2 \rangle \varepsilon_3 \quad (3)$$

In the second failure criteria, failure was projected to occur per Equation 4:

$$\left[\frac{1}{2S_tS_c}\right]\left[(\sigma_1-\sigma_2)^2+(\sigma_1-\sigma_3)^2+(\sigma_2-\sigma_3)^2\right]+\left[\left(\frac{1}{S_t}-\frac{1}{S_c}\right)(\sigma_1+\sigma_2+\sigma_3)\right]=1 \quad (4)$$

In the third failure criteria, failure was predicted to occur in accordance with Equation 5:

$$\left(\frac{\sigma_1}{S_t}-\frac{\sigma_3}{S_c}\right)=1 \quad (5)$$

Where: ε_1, ε_2, ε_3: are the first, second, and third principal strains, respectively

σ_1, σ_2, σ_3: are the first, second, and third principal stresses, respectively

S_t: ultimate tensile strength

S_c: ultimate compression strength

Relaxed Fall Configuration

Figures 3(a) and 4(a) show that there were higher stresses in the region of the femur's neck compared to the neighboring regions. The same can be said in the case of strains in Figures 3(b) and 4(b). The stress values in the relaxed (ρ = 2.0 g/cm³) were higher than that in relaxed (ρ = 1.5 g/cm³). However, the strain values in relaxed (ρ = 1.5 g/cm³) were higher than that in relaxed (ρ = 2.0 g/cm³). Figure 5 shows the failure in the femur's neck based on the failure criteria presented in Equation 5. It is clear that bone density highly affects failure; the lower the density values, the higher the potential for failure.

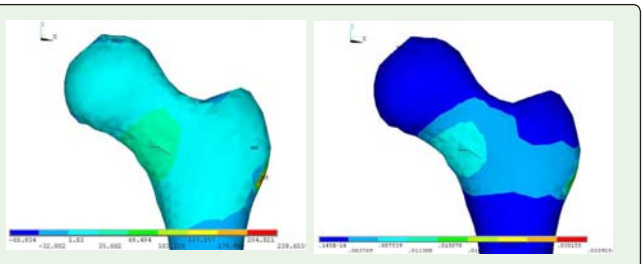

Figure 3: (a) First principal stress, (b) First principal strain, Relaxed configuration (ρ= 1.5 g/cm³).

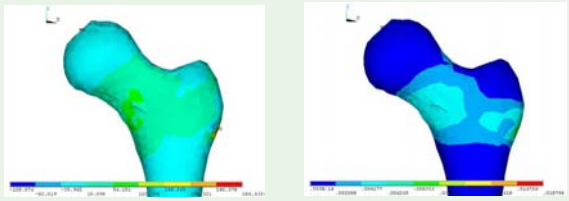

Figure 4: (a) First principal stress, (b) First principal strain Relaxed configuration (ρ = 2.0 g/cm³).

It can be shown that the same behavior exists in the other fall configurations, i.e. slap fall and tensed fall. From the figures shown above, there were high stresses and strains in the femur's neck. The peak values of stresses and strains for the similar paths coincide at the same location. All the paths follow the same pattern. From the failure figures, it is obvious that the failed zones follow the same pattern, and are located at the same neck location.

As shown in Tables 5 and 6 below, the highest stresses and strains were located at the medial path, followed by the anterior path. For the four different paths, the highest stresses and strains occurred in the tensed fall configuration, followed by the relaxed, and then the slap fall configuration. In all cases, it is evident that the stresses increased slightly, but the strains decreased significantly when the density was changed from low to high. This can be explained; the stresses are geometrically dependent, which is not changing much, while the strains are modulus and density dependent, which is changing significantly. The slight difference in the stresses between one case and another was due to the dependency on the applied loads. While the strains are highly dependent on material properties (modulus of elasticity and bone density), which are varying significantly between one model to another.

Table 5: Stress and strain comparison for all fall configurations/ Different densities (Anterior).

Anterior Side				
r (g/cm³)	1.5	1.7	1.8	2.0
Case	σ_1 (N/mm²)			
Relaxed	36.93	39.03	40.04	42.04
Slap	33.49	35.4	36.32	38.17
Tensed	37.89	40.05	41.08	43.18
	ε_1 (mm/mm)			
Relaxed	6.32E-03	4.99E-03	4.48E-03	3.63E-03
Slap	5.73E-03	4.53E-03	4.06E-03	3.30E-03
Tensed	6.48E-03	5.12E-03	4.60E-03	3.73E-03

Table 6: Stress and strain comparison for all fall configurations/ Different densities (Medial).

Medial Side				
r (g/cm³)	1.5	1.7	1.8	2.0
Case	σ_1 (N/mm²)			
Relaxed	49.22	50.03	50.34	50.78
Slap	44.65	45.38	45.66	46.06
Tensed	50.51	51.33	51.65	52.1
	ε_1 (mm/mm)			
Relaxed	9.02E-03	7.18E-03	6.47E-03	5.32E-03
Slap	8.18E-03	6.51E-03	5.87E-03	4.82E-03
Tensed	9.25E-03	7.36E-03	6.63E-03	5.46E-03

Conclusions

The critical fracture region from this analysis was the neck of the femur in all the cases investigated. The tensed fall configuration was the most critical case, followed by the relaxed, and then the slap configuration. This was due to the fact that for the tensed configuration impact loads applied to the femur's head were the highest. The stresses and strains that were obtained from the paths generated around the femur's neck (A, L, M, and P) followed the same pattern. The maximum values of the first principal stresses in the anterior and medial paths occurred at the same location. The maximum values of the third principal strains in the lateral and posterior occurred in the same location for all three fall configurations. The number of failed zones varied from one fall configuration to another for the same bone density. This variation was because the magnitude of the applied load was different from one configuration to another. The number of failed zones also changed for the same fall configuration (same load), due to the difference in the bone density. With the increase of the density, the likelihood of femur's neck fracture was decreased significantly for the same fall configuration.

References

1. Currey JD. Bones structures and mechanics. 1st edn. 2002.
2. Milovanovic P, Potocnik J, Djonic D, Nikloic S, Zivkovic V, Djuric M, et al. Age-related deterioration in trabecular bone mechanical properties at material level: Nanoindentation study of femoral neck in women by using AFM. Journal of Experimental Gerontology. 2012; 47: 154-159.
3. Bredella MA, Lin E, Gerweck AV, Landa MG, Thomas BJ, Torriani M, et al. Determinants of Bone Microarchitecture and Mechanical Properties in Obese Men. The Endocrine Society. 2012; 9: 4115-4122.
4. Koletsi D, Eliades T, Zinelis S, Bourauel C, Eliades G. Disease and functional loading effect on the structural conformation and mechanical properties of the mandibular condyle in a transgenic rheumatoid arthritis murine model: an experimental study. European Journal of Orthodontics. 2016; 38: 615-620.
5. Taylor WR, Ronald E, Ploeg H, Hertig D, Klabunde R, Warner MD, et al. Determination of orthotropic one elastic constants using FEA and modal analysis. Journal of Biomechanics. 2002; 35: 767-773.
6. Stain MS, Thomas CDL, Feik SA, Wark JD, Clement JG. Bone size and mechanics at the femoral diaphysis across age and sex. Journal of Biomechanics. 1998; 31: 1101-1110.
7. Keyak JH, Skinner HB, Fleming JA. Effect of force direction on femoral fracture load for two types of loading conditions. Journal of Biomechanics. 2001; 19: 539-544.
8. Keyak JH, Rossi SA. Prediction of femoral fracture load using finite element models: an examination of stress-based failure theories. Journal of Biomechanics. 2000; 33: 209-214.
9. Sabick MB, Hay JC, Goel VK, Banks SA. Active response decrease impact forces at the hip and shoulders in falls to the side. Journal of Biomechanics. 1999; 32: 993-998.
10. Morgan EF, Keaveny TM. Dependence of yield strain of human trabecular bone on anatomic site. Journal of Biomechanics. 2001; 34: 569-577.
11. ANSYS user manual version 7.0. 2003.
12. Viceconti M, Casali M, Massari B, Cristofolini L, Bassini S and Toni A. Standardized femur program, Proposal for reference geometry to be used for the creation of finite element models of the femur. Journal of Biomechanics. 1996; 29: 1241.
13. Rahman A. Finite element analysis and shape optimization of hip joint prosthesis with muscle forces. University of Wisconsin-Madison. 1993.

14. Wirtz DC, Schiffers N, Pandorf T, Radermacher K, Weichert D, Forst R. Critical evaluation of known bone material properties to realize anisotropic FE-simulation of the proximal femur. Journal of Biomechanics. 2000; 33: 1325-1330.

15. Gardner TN, Stoll T, Marks L, Mishra S, Knothe TM. The influence of mechanical stimulus on the pattern of tissue differentiation in a long bone fracture – an FEM study. Journal of Biomechanics. 2000; 33: 415-425.

16. Kaneko TS, Pejcic MR, Tehranzadeh J, Keyak JH. Relationships between material properties and CT scan data of cortical bone with and without metastatic lesions. Medical Engineering and Physics. 2003; 25: 445-454.

17. Lener Amy L, Kuhn Janet L, Hollister Scott J. Are regional variations in bone growth related to mechanical stress and strain parameters? Journal of Biomechanics. 1998; 31: 327-335.

18. Logan Daryl L. A first course in finite element methods. 3rd edn. 2002.

19. Smeesters, Cecile, Hayes,Wilson C., McMahon, Thomas A. Disturbance type and gait speed affect fall direction and impact location. Journal of Biomechanics. 2001; 34: 309-317.